Weierstraß-Institut
für Angewandte Analysis und Stochastik

im Forschungsverbund Berlin e.V.

Preprint ISSN 0946 – 8633

Stochastic Eulerian model for the flow simulation in porous media. Unconfined aquifers

Dmitry Kolyukhin [1] and Karl Sabelfeld [1,2]

submitted: 23rd March 2004

[1] Weierstrass Institute for Applied Analysis and Stochastics
Mohrenstraße 39
D – 10117 Berlin
Germany
E-Mail: sabelfeld@wias-berlin.de

[2] Institute of Computational Mathematics and Mathematical Geophysics
Russian Acad. Sci.
Lavrentieva str., 6
630090 Novosibirsk
Russia

No. 912
Berlin 2004

1991 *Mathematics Subject Classification.* 65C05, 76N20.

Key words and phrases. Hydraulic conductivity, Lognormal random field, small fluctuations, Darcy law, randomized spectral representation.

This work is supported partly by the RFBR Grant N 03-01-00914, HIII N 1271.2003.1, and NATO Linkage Grant N 978912.

Edited by
Weierstraß-Institut für Angewandte Analysis und Stochastik (WIAS)
Mohrenstraße 39
10117 Berlin
Germany

Fax: + 49 30 2044975
E-Mail: preprint@wias-berlin.de
World Wide Web: http://www.wias-berlin.de/

Abstract

This work deals with a stochastic unconfined aquifer flow simulation in statistically isotropic saturated porous media. This approach is a generalization of the 3D model we developed in [13]. In this paper we deal with a 2D model obtained via depth-averaging of the 3D model. The average hydraulic conductivity is assumed to be a random field with a lognormal distribution. Assuming the fluctuations in the hydraulic conductivity to be small we construct a stochastic Eulerian model for the flow as a Gaussian random field with a spectral tensor of a special structure derived from Darcy's law. A randomized spectral representation is then used to simulate this random field. A series of test calculations confirmed the high accuracy and computational efficiency of the method.

1 Introduction

The main difficulty in evaluation of pollutant transport in porous medium such as, for instance, aquifers is the extreme heterogeneity of the media. The parameters which locally describe the transport can be obtained in experiments, but they cannot be simply used to characterize the transport on large scales. Here we have a classical situation where there is a lack of knowledge on the local details of the spatial structure, but without this structure details it is not possible to describe the large scale behaviour. A natural approximation is based on the stochastic approach: the heterogeneities are modelled as random fields with given statistical properties. In hydrogeology this approach is often used, see, e.g., [6], [24] for the flow analysis in saturated zone, or [9], [18], [10], [4] for the transport of a dissolved pollutant in a saturated aquifer; see also overview in the books [5] and [11]. Stochastic approach allows for variations in other local properties, e.g., the hydraulic conductivity and the chemical adsorption coefficient (see [7], [3]), or the degradation constant (see [12]). An asymptotic analysis is undertaken in [19] when comparing two different averaging procedures.

To our knowledge, in the porous media transport, only one type of stochastic models was used, namely, the Random Displacement Method (RDM) for the hydrodynamic dispersion equation. It should be stressed that RDM can be applied only if the displacement covariance tensor is known (e.g., from measurements, or numerical simulation), and cannot be applied if the functionals of interest are evaluated at times comparable with the characteristic correlation scale of the flow. In contrast, the Lagrangian stochastic models based on the tracking particles in a random velocity field extracted from numerical solution of the flow equation are free of these limitations, but the computational resources required are vast. In [17], the first Langevin type stochastic model in the form of a stochastic differential equation for the position and velocity is constructed. It is worth to mention that this approach is widely used in the atmospheric transport problems, e.g., see [15],[22].

In the present paper we further develop the random field simulation technique which allows us to constrtuct samples of the velocity field and to simulate the transport of a passive scalar in porous medium under assumption of small fluctuations of the hydraulic conductivity. We deal here with the unconfined aquifers. The feature of the flow in an aquifer we use is that it may be approximately viewed as a horizontal flow. Therefore under some conditions, we can consider the flow characteristics as averaged over the height and thus turn to a 2D flow model. Frequently such situation arises in the case of flow at regional scale [5]. Simulation of random fields is based on the spectral structure of the hydraulic conductivity. In [13] we have applied a similar approach to a steady flow in porous media in 3D case. A stochastic Eulerian and a combined Eulerian-Lagrangian models were also developed by us in [16] for the analysis of relative dispersion of two particles moving in a turbulent flow. A small-perturbation analysis which uses the Kraichnan simulation technique was made by Schwarze et al. [23].

2 Formulation of the problem

We consider a steady flow through saturated porous formation. For a stationary 3D flow, the specific discharge is determined by the Darcy law

$$\mathbf{q}^{3D}(\mathbf{x}) = \theta^{3D}(\mathbf{x})\mathbf{u}^{3D}(\mathbf{x}) = -K^{3D}(\mathbf{x})\nabla(\varphi^{3D}(\mathbf{x})) \tag{1}$$

where $\mathbf{q}^{3D}$ is the so-called Darcy's velocity, or specific discharge, $\mathbf{u}^{3D}$ is the pore velocity, θ^{3D}, the porosity, φ^{3D}, the hydraulic potential $\varphi^{3D} = \frac{p}{\rho g} + z$, p is the fluid pressure, z is the height and K^{3D} - is the hydraulic conductivity assumed to be a homogeneous log-normal random field with a given spectral density.

Thus $\mathbf{q}^{3D}$ is a random field obtained from (1) where φ^{3D} is the solution of the following conservation of mass equation

$$\sum_{i=1}^{3} \frac{\partial}{\partial x_i}\left(K^{3D}(\mathbf{x})\frac{\partial \varphi^{3D}}{\partial x_i}\right) = 0\ . \tag{2}$$

The functions K^{3D} and θ^{3D} are the key parameters of the flow. Experimental measurements show high heterogeneous behaviour of K^{3D} in space with the following remarkable property: when considering K^{3D} as a random field, its distribution is well approximated by a log-normal law.

The porosity θ^{3D} is also often considered in some models as a random field. However its variability is in the problems we tackle generally much smaller than that of K^{3D}. We assume therefore $\theta^{3D}(\mathbf{x}) = \theta = const$.

In many groundwater-flows the vertical fluctuations are much less compared to the horizontal variations of the velocity field. To treat this description, the equations (1) and (2) are averaged over the vertical coordinate x_3 in order to derive an equation describing the two-dimensional aquifer flow. We will consider steady flow in unconfined aquifer with no recharge. This situation is described by equations [2], [11]:

$$\mathbf{q}(\mathbf{x}) = \theta \beta \mathbf{u}(\mathbf{x}) = -K(\mathbf{x})\beta\nabla(\varphi(\mathbf{x})) \,, \tag{3}$$

$$\sum_{i=1}^{2} \frac{\partial}{\partial x_i}\left(T(\mathbf{x})\frac{\partial\varphi}{\partial x_i}\right) = 0 \,, \tag{4}$$

here $\mathbf{q}$ is the integrated component of the specific discharge and it can be defined in words as volume of water per unit time and per unit length in the horizontal plane, and $\mathbf{u}$ is the depth-averaged pore velocity. The classical aquifer equation in the form (3), (4) treats only the depth-averaged flow conditions, and the head therein is a depth-averaged head. We use Dupuit assumption [2] that the equipotential surfaces are vertical (i.e., $\varphi =< \varphi(x_1, x_2) >$ is independent of x_3). Then in (3),

$$K(x_1, x_2) = \frac{1}{\beta}\int_0^{\beta(x_1,x_2)} K^{3D}(x_1, x_2, x_3)dx_3$$

is the average 2D hydraulic conductivity. The transmissivity T is formed as the product of K and β, the thickness of the aquifer:

$$T(x_1, x_2) = \beta(x_1, x_2)K(x_1, x_2) \,.$$

It has been assumed here that the transmissivity is a statistically isotropic in the plane.

In developing (3), (4), the head changes in the vertical are ignored which can be considered as a model in the case of small variation of the changes in the vertical.

We will consider the hydraulic log-conductivity $\ln K = F + f$ as a statistically homogeneous random field with gaussian distribution $N(m_f, \sigma_f)$. Here $m_f = F$, and σ_f is the standard deviation.

We assume small random perturbations about the mean values for the transmissivity,

$$\ln T = Y + y \,,$$

depth-averaged potential, specific discharge and pore velocity components:

$$\varphi =< \varphi > +\varphi' = H + h \,, \quad q_i =< q_i > +q_i', \quad u_i =< u_i > +u_i', \quad i = 1, 2 \,.$$

3 Spectrum of the specific discharge

We deal with statistically homogeneous random fields, and use the Fourier-Stiltjes representations, in particular,

$$f(\mathbf{x}) = \int\int exp(i(\mathbf{k}, \mathbf{x}))dZ_f(\mathbf{k})$$

$$h(\mathbf{x}) = \int\int exp(i(\mathbf{k}, \mathbf{x}))dZ_h(\mathbf{k})$$

$$u'_j(\mathbf{x}) = \int\int exp(i(\mathbf{k},\mathbf{x}))dZ_{u_j}(\mathbf{k}),$$

where $\mathbf{k} = (k_1, k_2)$ is the wave number vector, $\mathbf{x} = (x_1, x_2)$ is the position vector, and the integration is over two-dimensional wave number space.

We assume that $\ln K$ is statistically homogeneous and isotropic with the spectrum [11]:

$$S_{ff}(\mathbf{k}) = \sigma_f^2\alpha^2/[\pi(\alpha^2 + k^2)^2]; \quad k = |\mathbf{k}| \tag{5}$$

with the corresponding covariance function

$$C_{ff}(\mathbf{r}) = \sigma_f^2 \alpha r K_1(\alpha r); \quad r = |\mathbf{r}|; \quad \alpha = 1.65/I_f$$

where K_1 is the modified Bessel function, and I_f is the correlation length.

Assuming small perturbations ($\sigma_f^2 << 1$) Gelhar [10] evaluated the specific discharge spectrum using Darsy's law with isotropic hydraulic conductivity

$$u_j = -\frac{K}{\theta}(\partial\varphi/\partial x_j) = -\frac{K_G}{\theta}exp(f)(\partial\varphi/\partial x_j) = -\frac{K_G}{\theta}[1 + f + f^2 + ...](\partial H/\partial x_j + \partial h/\partial x_j) \tag{6}$$

where $K_G = exp(F)$.

Under small perturbation and dropping products of perturbed quantities, the mean-removed form of (6) is

$$u'_j = -\frac{K_G}{\theta}[f(\partial H/\partial x_j) + \partial h/\partial x_j]$$

and using the above Fourier-Stiltjes representation yields

$$dZ_{u_j} = \frac{K_G}{\theta}(J_j dZ_f - ik_j dZ_h) \tag{7}$$

where $J_j = -\partial H/\partial x_j$ - is the mean hydraulic gradient in x_j direction, $\mathbf{J} = (J_1, J_2)$.

The following relation follows from (4) (e.g., see [1])

$$\nabla^2 h = J_j(\partial y/\partial x_j). \tag{8}$$

Indeed, by (4) we find that

$$\frac{\partial^2\varphi}{\partial {x_j}^2} + \frac{\partial \ln T}{\partial x_j}\frac{\partial\varphi}{\partial x_j} = 0; \quad T \neq 0,$$

and taking the expected values we get

$$\frac{\partial^2 H}{\partial {x_j}^2} + \frac{\partial Y}{\partial x_j}\frac{\partial H}{\partial x_j} + \left\langle\left[\frac{\partial y}{\partial x_j}\frac{\partial h}{\partial x_j}\right]\right\rangle = 0\ .$$

After subtracting this from the original flow equation (4) we come to the following equation:

$$\frac{\partial^2 h}{\partial {x_j}^2} + \frac{\partial Y}{\partial x_j}\frac{\partial h}{\partial x_j} + \frac{\partial y}{\partial x_j}\frac{\partial H}{\partial x_j} = \left\langle \left[\frac{\partial y}{\partial x_j}\frac{\partial h}{\partial x_j} \right] \right\rangle - \frac{\partial y}{\partial x_j}\frac{\partial h}{\partial x_j} \approx 0.$$

From this, due to the small fluctuation assumption, we ignore the products of fluctuations, and since the random field Y is homogeneous, $\frac{\partial Y}{\partial x_j} = 0$, we come to the formula (8):

$$\frac{\partial^2 h}{\partial {x_m}^2} = J_m \frac{\partial y}{\partial x_m}.$$

The perturbation in $\ln T$ [11] can be written as

$$y = \ln K\beta - \langle \ln K\beta \rangle = f + \ln(1 + \frac{b}{B}) \approx f + \frac{b}{B} = f + \frac{h}{B} \ ;$$

$$\beta = B + b \ , \quad \langle b \rangle = 0 \ , \quad \beta = \varphi - L = H + h - L$$

where $f = \ln K/K_G$. In the second line, it has been assumed that the fluctuation in aquifer thickness, b is small compared to the mean aquifer thickness B. It has also been assumed that the bottom elevation of the aquifer, L is known precisely.

Then

$$\frac{\partial^2 h}{\partial {x_m}^2} - \frac{J_m}{B}\frac{\partial h}{\partial x_m} = J_m \frac{\partial f}{\partial x_m}.$$

From this one finds

$$dZ_h = \frac{-iJ_m k_m}{k^2 + i\frac{J_m k_m}{B}} dZ_f, \tag{9}$$

hence,

$$dZ_{u_j} = \frac{K_G}{\theta}\left(J_j - \frac{k_j B J_m k_m (k^2 B - iJ_m k_m)}{k^4 B^2 + (J_m k_m)^2} \right) dZ_f$$

which implies

$$\begin{aligned} S_{u_j u_l}(k) = \langle \overline{dZ_{u_j}} dZ_{u_l} \rangle = \frac{K_G^2}{\theta^2} \overline{\left(J_j - \frac{k_j B J_m k_m (k^2 B - iJ_m k_m)}{k^4 B^2 + (J_m k_m)^2} \right)} \times \\ \left(J_l - \frac{k_l B J_n k_n (k^2 B - iJ_n k_n)}{k^4 B^2 + (J_n k_n)^2} \right) S_{ff}(k), \quad m, n = 1, 2 \ . \end{aligned} \tag{10}$$

Under small perturbation assumptions the velocity is modelled as

$$\mathbf{u}(\mathbf{x}) = < \mathbf{u}(\mathbf{x}) > + \mathbf{u}'(\mathbf{x}) \approx K_G \mathbf{J}/\theta + \mathbf{u}'(\mathbf{x}) \ .$$

4 Simulation of specific discharge perturbation random field

The spectral tensor $S(\mathbf{k})$ takes the form

$$S_{jl}(\mathbf{k}) = \overline{a_j(\mathbf{k})}a_l(\mathbf{k}) \tag{11}$$

where

$$a_j(\mathbf{k}) = \frac{K_G}{\theta}\left(J_j - \frac{k_j B J_m k_m (k^2 B - i J_m k_m)}{k^4 B^2 + (J_m k_m)^2}\right)(S_{ff}(\mathbf{k}))^{1/2} \ .$$

Now we present simulation formulae in the case of real-valued random field with the spectral tensor $\{S_{jl}(\mathbf{k})\}$, see [21].

Let $p(\mathbf{k})$ be an arbitrary density function defined on the same wave number space of $\mathbf{k}$.

Sample $\mathbf{k}$ according to $p(\mathbf{k})$ and let ξ_k and η_k be mutually independent random variables with zero mean and unit variance, independent of $\mathbf{k}$.

Let

$$\boldsymbol{\xi}'_k(\mathbf{a}) = \xi_k\, Re(\mathbf{a}(\mathbf{k})) - \eta_k\, Im(\mathbf{a}(\mathbf{k}))\ , \quad \boldsymbol{\eta}'_k(\mathbf{a}) = \xi_k\, Im(\mathbf{a}(\mathbf{k})) + \eta_k\, Re(\mathbf{a}(\mathbf{k}))\ .$$

Then we construct the vector random field

$$\mathbf{u}(\mathbf{x}) = \frac{1}{\sqrt{p(\mathbf{k})}}\left(\boldsymbol{\xi}'_k(\mathbf{a})\cos(\mathbf{k},\mathbf{x}) + \boldsymbol{\eta}'_k(\mathbf{a})\sin(\mathbf{k},\mathbf{x})\right)\ .$$

Here $\mathbf{k}$ is sampled accoding to the density $p(\mathbf{k})$ which is, generally, an arbitrary density function which can be chosen from rather different arguments. For instance, it is recommended in [21], to use $p(\mathbf{k}) = a^2(\mathbf{k})/\int_{R^3} a^2(\mathbf{k})d\mathbf{k}$. We take $p(\mathbf{k}) = S_{ff}(\mathbf{k})/\int_{R^3} S_{ff}(\mathbf{k})d\mathbf{k}$.

It is easy to verify that

$$\langle \boldsymbol{\xi}'_k(\mathbf{a})\boldsymbol{\xi}'_k(\mathbf{a})|\mathbf{k}\rangle = \langle \boldsymbol{\eta}'_k(\mathbf{a})\boldsymbol{\eta}'_k(\mathbf{a})|\mathbf{k}\rangle = S(\mathbf{k}),$$

and

$$\langle \boldsymbol{\xi}'_k(\mathbf{a})\boldsymbol{\eta}'_k(\mathbf{a})|\mathbf{k}\rangle = 0$$

by definition. Using these properties, it is possible to show that the random field $\mathbf{u}$ has the desired spectral tensor $\{S_{jl}(\mathbf{k})\}$.

We have described the simulation of a random field with zero mean $\overline{\mathbf{u}(\mathbf{x})} = 0$ and with a given spectral tensor $S(\mathbf{k})$, where no assumption about multidimensional distributions of the random field have been made. In the case of gaussian random fields the algorithm can be modified as follows. We simulate $i = 1, 2, \ldots N$ independent random fields with $S(\mathbf{k})$, then we set

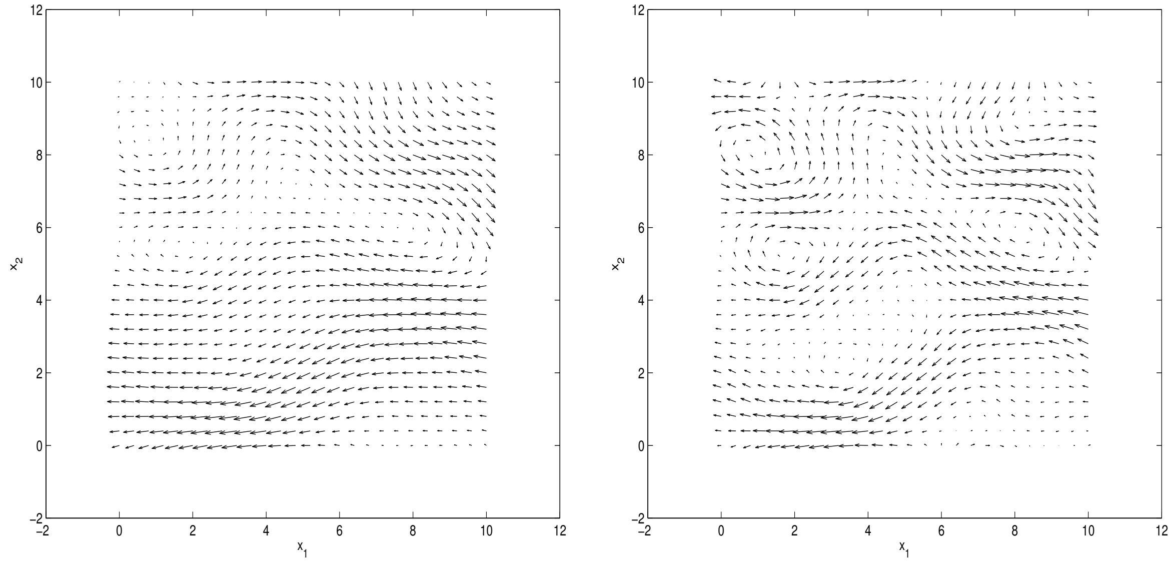

Figure 1: Samples of specific discharge perturbation random fields u'_1, u'_2, for the isotropic hydraulic conductivity. Left picture: $\alpha = 0.6$, right picture: $\alpha = 2.0$. The number of harmonics was $N = 100$.

$$\mathbf{u}^{(N)}(\mathbf{x}) = \frac{1}{\sqrt{N}} \sum_{i=1}^{N} \left[\frac{1}{\sqrt{p(\mathbf{k}_i)}} \left(\boldsymbol{\xi}'_{ki}(\mathbf{a}) \cos(\mathbf{k}_i, \mathbf{x}) + \boldsymbol{\eta}'_{ki}(\mathbf{a}) \sin(\mathbf{k}_i, \mathbf{x}) \right) \right]$$

where

$$\boldsymbol{\xi}'_{ki}(\mathbf{a}) = \xi_{ki}\, Re(\mathbf{a}(\mathbf{k}_i)) - \eta_{ki}\, Im(\mathbf{a}(\mathbf{k}_{ki}))\ , \quad \boldsymbol{\eta}'_{ki}(\mathbf{a}) = \xi_{ki}\, Im(\mathbf{a}(\mathbf{k}_i)) + \eta_{ki}\, Re(\mathbf{a}(\mathbf{k}_{ki}))\ .$$

and $\mathbf{k}_i$, ξ_{ki}, η_{ki} are all sampled independently.

The central limit theorem ensures, under some general assumption [14], that $\mathbf{u}^{(N)}(\mathbf{x})$ converges to an ergodic gaussian random field with the spectral tensor $S(\mathbf{k})$, as $N \to \infty$.

5 Testing the simulation procedure

In this section we present some results of simulation, in particular, we show examples of the discharge field samples with the given spectrum, and compare the simulation results against the exact solutions. The hydraulic log-conductivity $\ln K$ is assumed to be normal with the mean $F = 3.4012$ and the spectrum (5). The mean hydraulic gradient is fixed as $\mathbf{J} = (J, 0)$, $J = 0.01$, $\sigma_f^2 = 0.01$. The mean thickness of the aquifer $B = 1$.

For illustration, we present in Figure 1, one sample of specific discharge perturbation random field u'_1, u'_2, in the region (x_1, x_2).

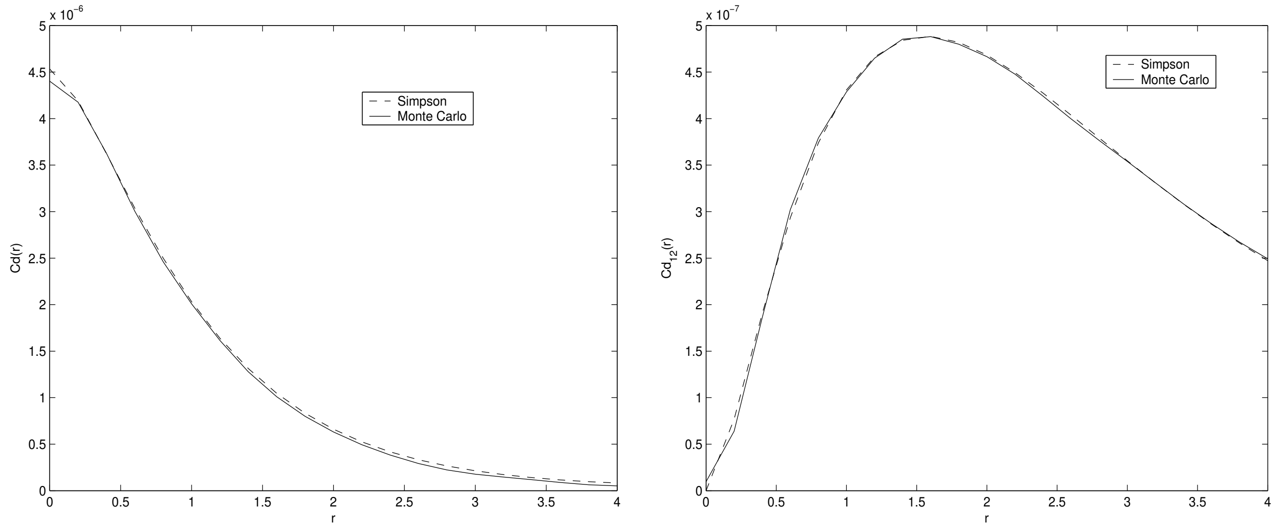

Figure 2: The functions $Cd(r)$ (left picture) and $Cd_{12}(r)$ (right picture).

5.1 Comparison with exact results

For testing our model we calculate the correlation functions

$$C_{jl}(\mathbf{r}) = \langle u_j(\mathbf{x}) u_l(\mathbf{x} + \mathbf{r}) \rangle$$

by using Monte Carlo simulation and compare them with the results of numerical integration

$$C_{jl}(\mathbf{r}) = \int_{R^2} S_{jl}(\mathbf{k}) e^{i(\mathbf{r},\mathbf{k})} d\mathbf{k} \ . \tag{12}$$

The expectation was calculated as an arithmetic mean over $N = 10^7$ samples, while the Simpson's rule was used to evaluate the integral (12).

Let us consider the correlations along the diagonal, i.e., let $Cd_{jl}(r) = \langle u_j(0,0) u_l(r,r) \rangle$.

In Figure 2 we plot the function $Cd(r) = Cd_{11}(r) + Cd_{22}(r)$ and the cross correlations Cd_{12}, $\alpha = 1$.

The error of calculations is very small, and the curves almost coincide, so that it is hard to see the difference between the curves in both pictures. Of course, the error is relatively larger for small correlations.

5.2 Spatial structure of the velocity field

Before presenting the calculations for the Eulerian correlation functions of the velocity field, let us make a remark on a similarity property of these functions.

The statistical characteristics of our problem, e.g., the correlation tensor C_{jl}, depend on many parameters, especially on the depth B and the correlation length I_f. However it can be shown that C_{jl} depends only on the ratio I_f/B which essentially simplifies the analysis.

Indeed, in the new coordinates $k_i' = k_i I_f$, $I_f' = I_f/B$, $r' = r/I_f$ the spectral tensor (10) reads

$$
\begin{aligned}
S_{u_j u_l}(\mathbf{k}') = \frac{K_G^2}{\theta^2} & \overline{\left(J_j - \frac{k_j' J_m k_m' (k'^2 - i J_m k_m' I_f')}{k'^4 + (J_m k_m' I_f')^2} \right)} \\
& \left(J_l - \frac{k_l' J_n k_n' (k'^2 - i J_n' k_n' I_f')}{k'^4 + (J_n k_n' I_f')^2} \right) S_{ff}(k'), \quad m, n = 1, 2 \ .
\end{aligned} \tag{13}
$$

$$
S_{ff}(\mathbf{k}') = 2.7225 \times (I_f)^2 \sigma_f^2 / [\pi (2.7225 + k'^2)^2]; \quad k' = |\mathbf{k}'| \ ,
$$

hence

$$
C_{jl}(\mathbf{r}) = \int_{R^2} S_{jl}(\mathbf{k}) e^{i(\mathbf{r},\mathbf{k})} d\mathbf{k} = \int_{R^2} \frac{S_{jl}(\mathbf{k}')}{I_f^2} e^{i(\mathbf{r}',\mathbf{k}')} d\mathbf{k}' = C_{jl}(\mathbf{r}') \ .
$$

Thus in the new coordinates, $C_{jl}(\mathbf{r}')$ depends only on I_f'.

Note that rigorously, we cannot conclude from this that the Lagrangian correlation function has the same similarity property on I_f/B. However our calculations (see figures 6,7,8) show that this might be true, at least approximately. This agrees also with the well known approximation that the Eulerian and Lagrangian correlation functions are similar; see also [5].

For the spatial picture of the velocity field, it is convenient to present the following correlation functions:

$$
C_{22}(r_2) = \langle u_2(0)\, u_2(r_2) \rangle, \quad C_{22}(r_1) = \langle u_2(0)\, u_2(r_1) \rangle
$$

for the transversal correlation function in the transversal and longitudinal directions, respectively.

Analogously, for the longitudinal velocity the functions $C_{11}(r_1)$ and $C_{11}(r_2)$ are defined.

We normalize these functions to unity at zero, and plot the curves as functions on r/I_f.

The longitudinal component shows a monotone decay in the longitudinal direction, with a predictable dependence on the height B: for smaller heights the correlation length is smaller (left picture in Figure 3).

More interesting is the behaviour of the transversal component in the longitudinal direction (right picture in Figure 3): here we see a region where this function is negative, and

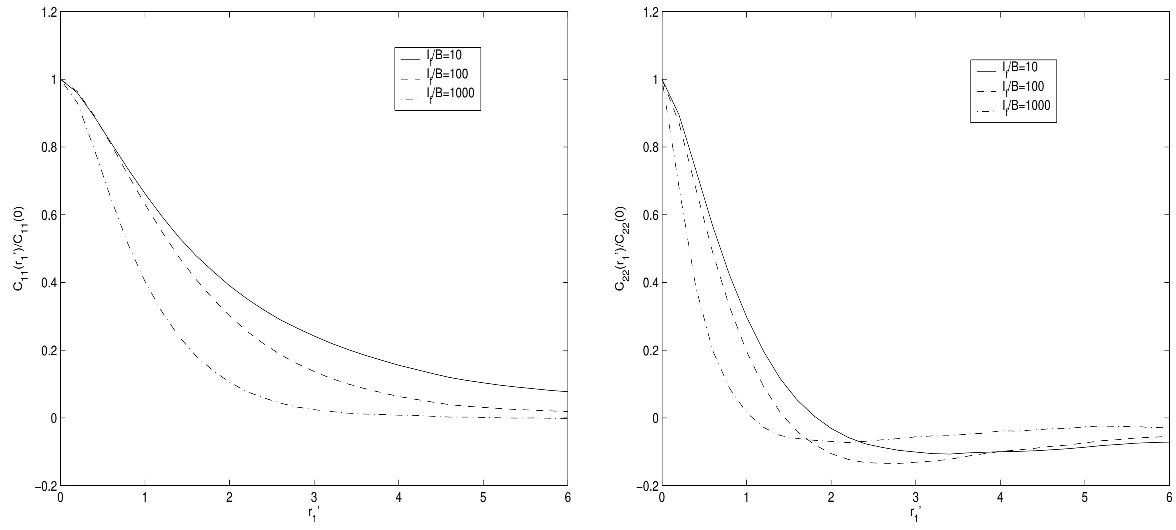

Figure 3: The longitudinal $C_{11}(r_1/I_f)$ and transverse $C_{22}(r_1/I_f)$ correlation coefficients as functions of the longitudinal coordinate.

this happens for all heights. This implies that the decorrelation is achieved through a transversal random walk in both directions.

As seen from Figure 4, right picture, for all heights of the layer, the transversal correlations in transversal direction have a large negative part which implies that the vortices move in the transversal direction quite symmetrically, with a characteristic size which can be estimated from this curve (being smaller for smaller heights).

Longitudinal velocity component in transversal direction (Figure 4, left picture) has a longer correlation length, and negative values appear only for small heights.

Remark.

The spectrum (10) is derived under the assumptions $\sigma_f << 1$ and $b << B$. In Figure 5 we show the results of numerical calculations of functions σ_h/I_f and σ_h/B, where σ_h is the standard deviation of the hydraulic potential ϕ (recall that $\phi = H + h$). It is seen that σ_h/B grows from 10^{-6} for small values of I_f/B, and then slowly approaches 10^{-2} in the interval $I_f/B > 1$.

These results can be used to analyse the assumption $b << B$. Note that the two lower curves have good agreement with the head-variance relationship

$$\sigma_h^2 = 0.37\sigma_f^2 J^2 I_f^2 \ln(1.21B/JI_f) \; ; \quad JI_f/B << 1 \; ,$$

founded by Gelhar [8] for the two-dimensional case and spectrum (5).

6 Lagrangian statistical characteristics

In this section we present the results of numerical simulations for some Lagrangian statistical characteristics of the flow.

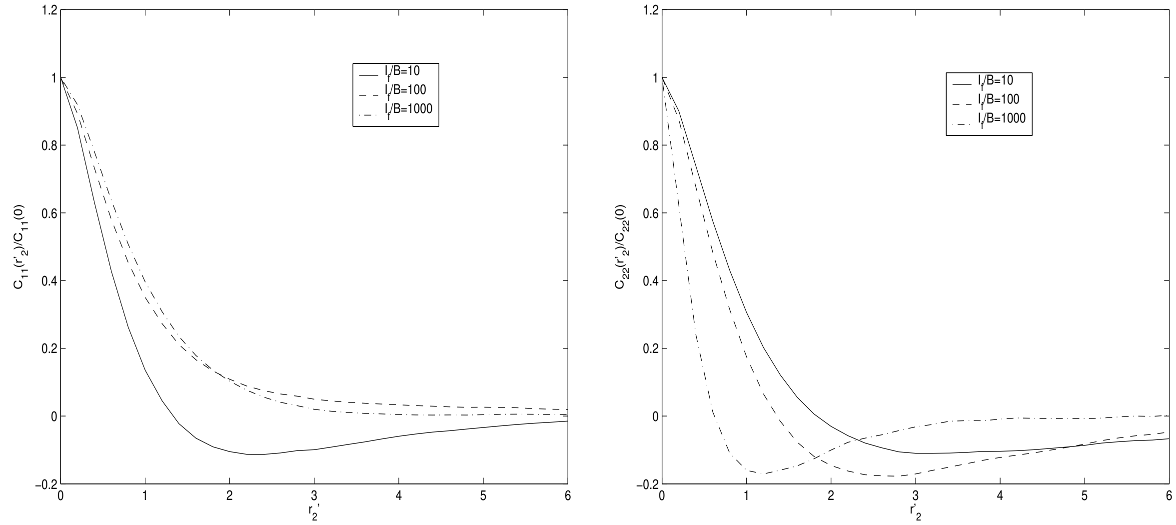

Figure 4: The longitudinal $C_{11}(r_1/I_f)$ and transverse $C_{22}(r_1/I_f)$ correlation coefficients as functions of the transverse coordinate.

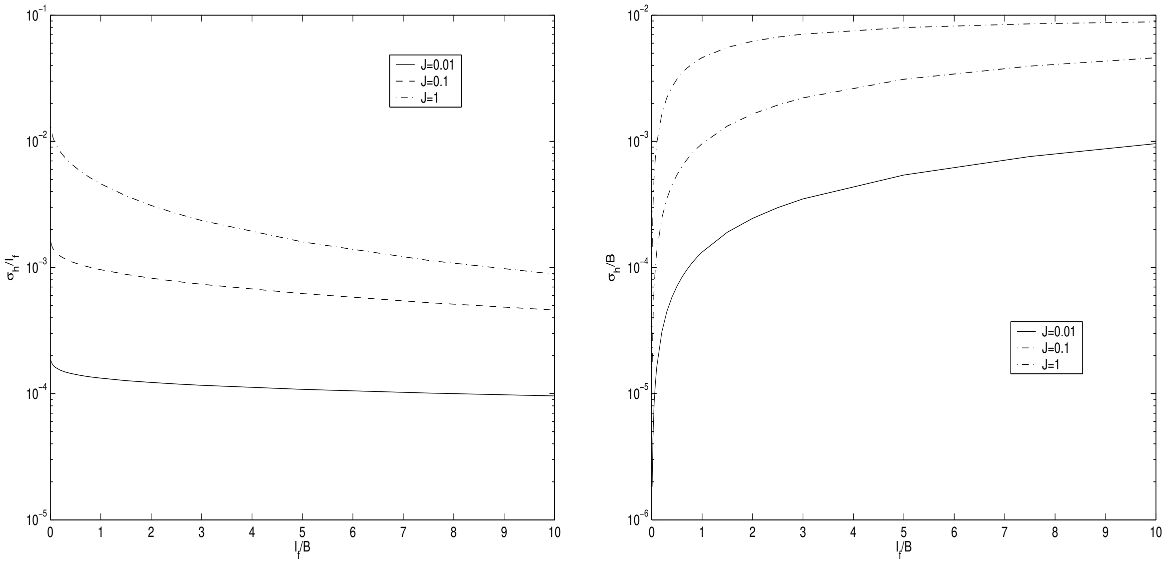

Figure 5: Monte Carlo calculations of functions σ_h/I_f and σ_h/B in unconfined aquifer.

In simulations, $\ln K$ was taken as an isotropic gaussian random field with the mean $F = 3.4012$ and spectrum (5). The mean hydraulic gradient is again fixed as $\mathbf{J} = (J, 0)$, $J = 0.01$, $\sigma_f^2 = 0.01$.

Recall now that we deal with a flow in which the head changes in the vertical are very small. Accordingly the vertical velocity and horizontal velocity changes in the vertical are also small. Thus let us introduce a Lagrangian trajectory $\mathbf{X}(t) = (X_1(t), X_2(t))$ starting at a point $\mathbf{x}_0$ as a function satisfying the equation:

$$\frac{d\mathbf{X}}{dt} = \mathbf{u}(\mathbf{X}), \quad \mathbf{X}(0) = \mathbf{x}_0 , \tag{14}$$

where $\mathbf{u}$ is here the depth-averaged pore velocity. It is assumed that the random velocity field $\mathbf{u}$ is smooth enough so that there exists a unique solution to (14) which is a vector random process with a mean $\langle \mathbf{X}(t) \rangle$.

The displacement covariances are defined by

$$D_{ij}(t) = \langle (X_i(t) - \langle X_i \rangle(t))(X_j(t) - \langle X_j \rangle(t)) \rangle .$$

In what follows we deal with the normalized dispersions:

$$D'_{ij} = D_{ij}/I_f^2, \quad i,j = 1,2$$

and dimensionless time $t' = t\,U/I_f$, where $U = K_G J/\theta$.

In Fig. 6, the functions $D'_{11}(t')/\sigma_f^2$ and $D'_{22}(t')/\sigma_f^2$ in unconfined aquifers are shown for various values I_f/B. The function $D'_{11}(t')/\sigma_f^2$ differs insignificantly for $I_f/B = 1$ and $I_f/B = 100$. The behaviour of $D'_{22}(t')/\sigma_f^2$ is more sensitive to the increasing of I_f/B.

Important Lagrangian characteristic is the Lagrangian correlation tensor of velocity:

$$R_{ij}(\tau) = \langle [(u_i(X(t)) - \langle u_i(X(t)) \rangle] \, [(u_j(X(t+\tau)) - \langle u_j(X(t+\tau)) \rangle] \rangle$$

where X is a Lagrangian trajectory started at the time t.

We have calculated $R_{11}(\tau)$ and $R_{22}(\tau)$, the Lagrangian correlation functions of the longitudinal and transverse velocities, respectively. In Figure 7 we plot these functions normalized by $R_{ii}(0)$, $i = 1, 2$. It should be noted that the further calculations for values of I_f/B smaller than 10 do almost not affect the curves after I_f/B reaches the value of 10. The limit correlation functions (as I_f/B goes to zero) corresponds to the ordinary diffusion behaviour. The same is true for the curves presented in Figures 3, 4 and 8.

Our calucations show a superdiffusion behaviour, as also reported in [13]: the transversal integral time scale defined as the integral of the transverse correlation function appears to be zero which makes impossible the application of the classical Taylor formula relating the dispersion with the integral of the correlation function. The long negative time correlations lead also to a trapping of particles and a non-Fickian behaviour of the transverse dispersion, see the right pictures of Figure 6.

Important Lagrangian statistical characteristics are the Lagrangian velocity structure functions defined as [20]

$$G_{ij}(t) = \langle \Delta V_i(t) \, \Delta V_j(t) \mid \mathbf{X}(t_0) = \mathbf{x}_0; \rangle , \qquad i,j = 1,2 ,$$

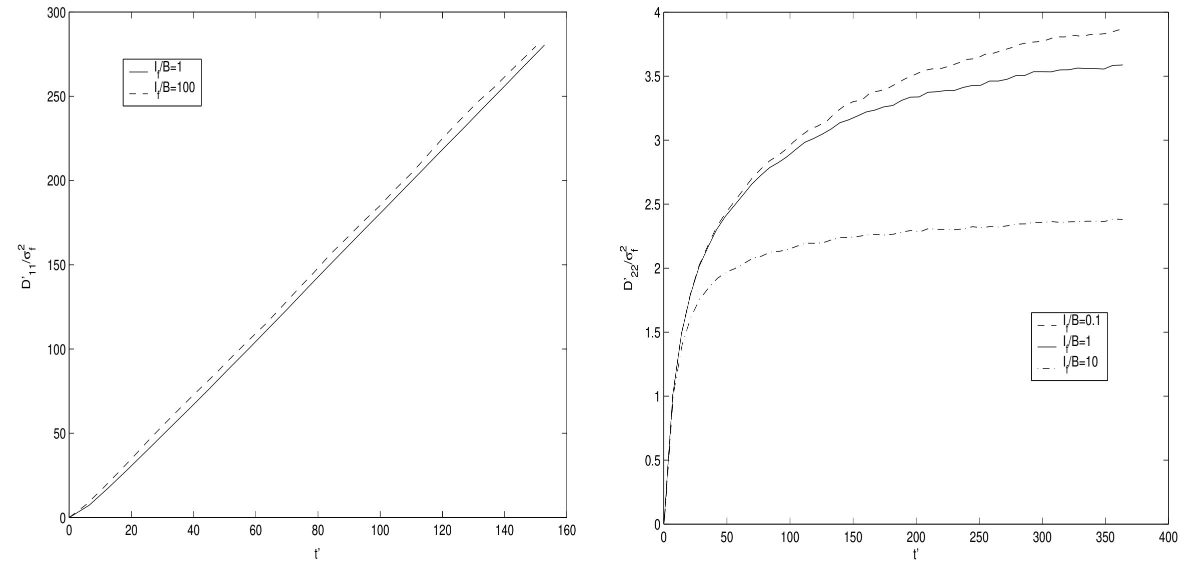

Figure 6: Monte Carlo calculations of functions D'_{11}/σ_f^2 and D'_{22}/σ_f^2 in unconfined aquifer are shown for various values I_f/B.

where $\Delta V_i(t) = u_i(\mathbf{X}(t; t_0, \mathbf{x}_0)) - u_i(t_0)$.

In Figure 8, we show the results of calculations of the longitudinal (left picture) and transverse (right picture) Lagrangian velocity structure functions, for three different values of I_f/B.

7 Conclusion

Stochastic Eulerian model for the unconfined aquifer flow in statistically isotropic porous media is constructed under the assumption of small fluctuations of the hydraulic conductivity, which is considered as a log-normal random field with a given spectral density, and under the Depuit shallow-water flow approximation. The randomized simulation approach developed in [21] is used to construct a vector field with a spectral tensor analitically derived from the stochastic Darcy equation. A series of test calculations confirmed the high accuracy and computational efficiency of the method. Calculations of the longitudinal and transverse dispersions, the Lagrangian correlation functions and the Lagrangian velocity structure functions have been carried out to extract the main statistical features of the flow. The calculations of the eulerian correlation tensor is simplified in dimensionless coordinates where it shows a similarity behaviour, so that it depends only on the ratio of the log-permeability correlation length to the mean depth of the flow.

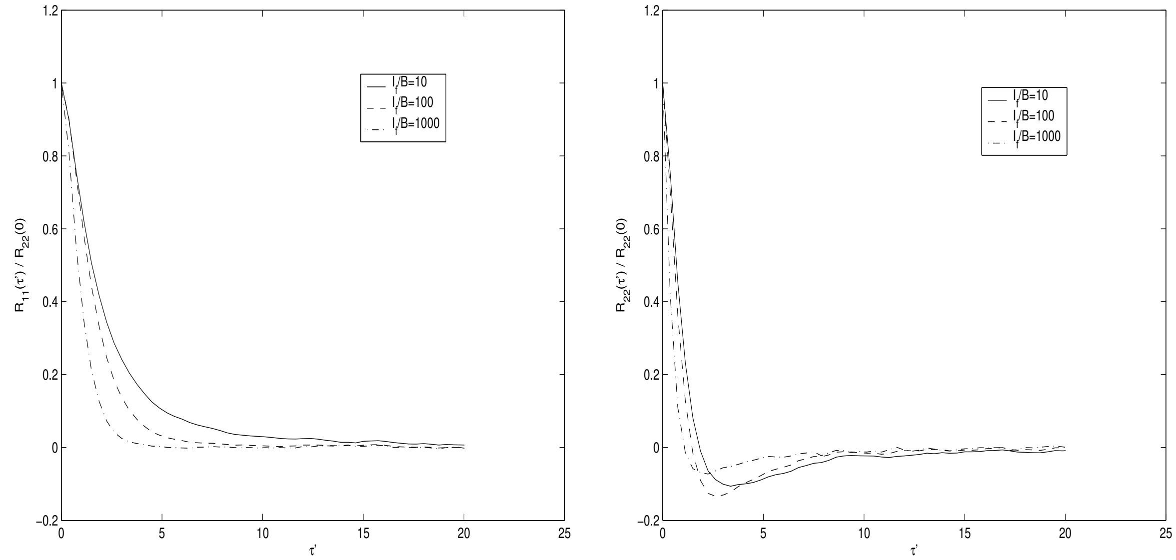

Figure 7: Longitudinal (left picture) and transverse (right picture) Lagrangian correlation functions of velocity.

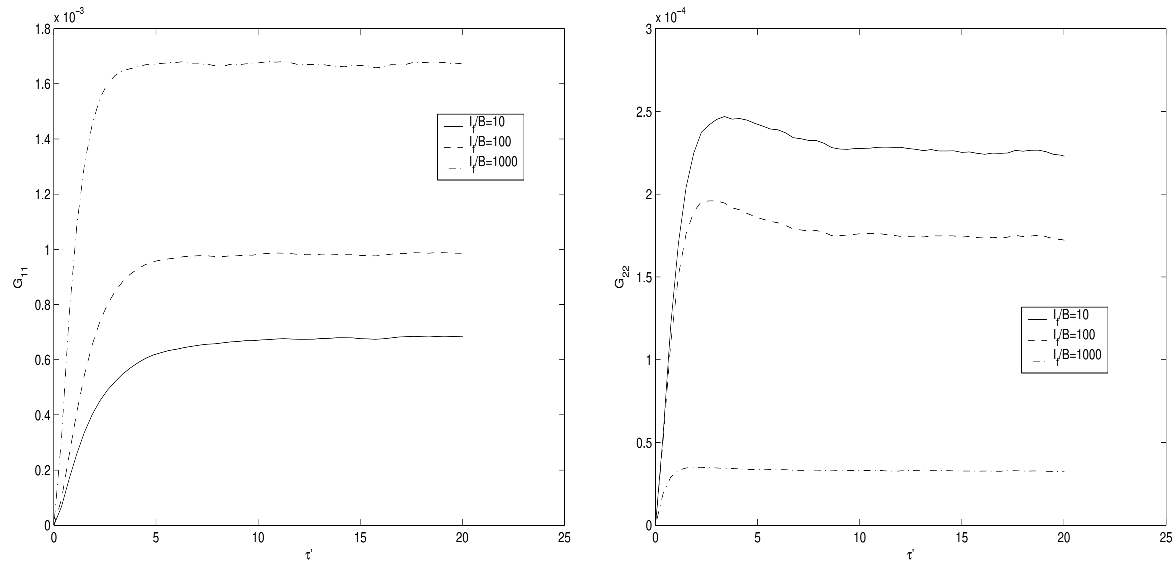

Figure 8: Longitudinal (left picture) and transverse (right picture) Lagrangian structure functions of velocity.

References

[1] Bark, A.A., L.W. Gelhar, A.L. Gutjahr, and J.R. MacMillan. Stochastic analysis of spatial variability in subsurface flows,1, Comparison of one- and three- dimensional flows. *Water Resour. Res.*, 14(2), 263-271, 1978.

[2] Bear, J., Dynamics of Fluids in Porous Media. American Elseviar, New York, 1972.

[3] Bellin A., Rinaldo A., Bosma W., van der Zee S., Rubin Y. Linear equilibrium adsorbing solute transport in physically and chemically heterogeneous porous formations. 1. Analytic solutions. *Water Resour. Res.*, 29, 4019-4031, 1993.

[4] Dagan G. Solute transport in heterogeneous porous formations. *J. Fluid Mech.*, 145, 151-177, 1984.

[5] G. Dagan. Flow and Transport in Porous Formation. Springer-Verlag. Berlin, Heidelberg, 1989.

[6] Freeze R.A. A stochastic-conceptual analysis of groundwater flow in non-uniform, homogeneous media. Water Resour. Res. 11(5), 725-741, 1975.

[7] Garabedian S.P., Gelhar L.W. and Celia M.A. Large-scale dispersive transport in aquifers: Field experiments and reactive transport theory. Parsons Laboratory Report 315, MIT, Cambridge, 1988.

[8] Gelhar L.W. Effects of hydraulic conductivity variations on groudwater flow, In Proceedings Second International Symposium on Stochastic Hydraulics, International Association for Hydraulic Research, Lund, Sweden, pp. 409-428, Water Resources Publications, Fort Collins, CO, 1977.

[9] Gelhar L.W., Gutjahr A.L. and Naff R.L. Stochastic analysis of macro-dispersion in a stratified aquifer. *Water Resour. Res.*, 19, 161-180, 1979.

[10] Gelhar, L.J., and C.L. Axness. Three-dimensional stochastic analysis of macrodispersion in aquifers. *Water Resour. Res.*, 19, 161-180, 1983.

[11] L.W. Gelhar. Stochastic Subsurface Hydrology. Englewood Cliffs, New Jersey: Prentice Hall, 1992.

[12] Kabala Z.J. and Sposito G. Stochastic model of reactive solute transport with time varying velocity in a heterogeneous aquifer. *Water Resour. Res.*, 27(3), 341-350, 1991.

[13] Karl Sabelfeld and Dmitry Kolyukhin. Stochastic Eulerian model for the flow simulation in porous media. *Monte Carlo Methods and Applications.* (2003), V.9, N.3, 271-290.

[14] O.A. Kurbanmuradov. Weak convergence of randomized spectral models of Gaussian random vector fields. *Bull. Nov. Comp. Center, Nim. Anal.*, 4 (1993), 19-25.

[15] Kurbanmuradov and K.K. Sabelfeld. Lagrangian stochastic models for turbulent dispersion in the atmospheric boundary layer. *Boundary-Layer Meteorology*, vol.97 (2000), 2, 191-218.

[16] O.Kurbanmuradov, K. Sabelfeld and D. Koluhin. Stochastic Lagrangian Models for Two-Particle Motion in Turbulent Flow. Numerical Results. *Monte Carlo Methods and Applications*. (1997), V.3, N.3, 199-224.

[17] Kurbanmuradov O., Sabelfeld K., Smidts O. and Vereecken H. A Lagrangian stochastic model for the transport in statistically homogeneous porous media. WIAS Preprint N786, 2002.

[18] Matheron and de Marsily. Is transport in porous media always diffusive? A counter example. *Water Resour. Res.*, 16(5), 901-917, 1980.

[19] Metzger D., Kinzelbach H., Neuweiler I. and Kinzelbach W. Asymptotic transport parameters in a heterogeneous porous medium: Comparison of two ensemble-averaging procedures. *Stochastic Environmental research and Risk Assesment*, 13, 396-415, 1999.

[20] A.S. Monin and A.M. Yaglom. *Statistical Fluid Mechanics: Mechanics of Turbulence*, Volume 2. The M.I.T. Press, 1981.

[21] K.K. Sabelfeld. Monte Carlo Methods in Boundary Value Problems. New York, 1991.

[22] Sabelfeld and O.A. Kurbanmuradov. One-particle stochastic Lagrangian model for turbulent dispersion in horizontally homogeneous turbulence. *Monte Carlo Methods and Applications*, vol.4 (1998), N2, 127-140.

[23] H. Schwarze, U. Jaekel and H. Vereecken. Estimation of Macrodispersion by Different Approximation Methods for Flow and Transport in Randomly Heterogeneous Media. *Transport in Porous Media*. (2001), V.49, N.2, 267-287.

[24] L. Smith and R.A. Freeze. Stochastic analysis of steady state groundwater flow in a bounded domain, 1. One-dimensional simulation. *Water Resour. Res.*, 15(3), 521-528, 1979.